A Journal of the Gesellschaft Deutscher Chemiker

Angewandte International Edition GDCh Chemie

www.angewandte.org

Accepted Article

Title: Regio- and Stereo-Selective Isomerization of Borylated 1,3-Dienes Enabled by Selective Energy Transfer Catalysis

Authors: Byeongseok Kweon, Lukas Blank, Julia Soika, Amélia Messara, Constantin Daniliuc, and Ryan Gilmour

To be cited as: *Angew. Chem. Int. Ed.* **2024**, e202404233

Link to VoR: https://doi.org/10.1002/anie.202404233

WILEY VCH

10.1002/anie.202404233

WILEY-VCH

RESEARCH ARTICLE

Regio- and Stereo-Selective Isomerization of Borylated 1,3-Dienes Enabled by Selective Energy Transfer Catalysis

Byeongseok Kweon,[a] Lukas Blank,[a] Julia Soika,[a] Amélia Messara,[a] Constantin G. Daniliuc[a] and Ryan Gilmour[a]*

[a] M.Sc. B. Kweon, M.Sc. L. Blank, M.Sc. Julia Soika, Dr. A. Messara, Dr. C. G. Daniliuc, Prof. Dr. R. Gilmour
University of Münster
Institute for Organic Chemistry
Corrensstraße 36, 48149 Münster (Germany)
E-mail: ryan.gilmour@uni-muenster.de
https://www.uni-muenster.de/Chemie.oc/gilmour/

Supporting information for this article is given via a link at the end of the document.

Abstract: Configurationally-defined dienes are pervasive across the bioactive natural product spectrum, where they typically manifest themselves as sorbic acid-based fragments. These C_5 motifs reflect the biosynthesis algorithms that facilitate their construction. To complement established biosynthetic paradigms, a chemical platform to facilitate the construction of stereochemically defined, functionalizable dienes by light-enabled isomerization has been devised. Enabled by selective energy transfer catalysis, a variety of substituted β-boryl sorbic acid derivatives can be isomerized in a regio- and stereo-selective manner (up to 99:1). Directionality is guided by a stabilizing $n_O \rightarrow p_B$ interaction in the product: this constitutes a formal *anti*-hydroboration of the starting alkyne. This operationally simple reaction employs low catalyst loadings (1 mol%) and is complete in 1 h. X-ray analysis supports the hypothesis that the $n_O \rightarrow p_B$ interaction leads to chromophore bifurcation: this provides a structural foundation for selective energy transfer.

Introduction

1,3-Dienes are ubiquitous in the bioactive small molecule repertoire,[1] where the stereochemical information encoded at the 2-dimensional level often manifests itself at the structure-function interface.[2] Frequently, these venerable units are part of a C_5-sorbic acid-based dienone motifs (Figure 1, top), thus reflecting the biosynthetic logic enables their generation.[3] Inspired by the importance of C_5 building blocks such as isopentenyl pyrophosphate (IPP) and dimethylallyl pyrophosphate (DMAPP) in biochemistry, it was envisaged that the creation of a suite of geometrically programmable sorbic acid derivatives with a C_5-chromophore, in which the alkene geometry could be inverted by light enabled isomerization (Fig. 1, middle),[4] would be enabling: this would allow natural product fragments to be accessed in a stereocontrolled manner and facilitate library development.[5] Furthermore, this would provide configurationally-defined C_5-modules for subsequent stereospecific transformations, where the relative stereochemistry of the product could be regulated by pre-defining the alkene configuration (Fig. 1, bottom).[6] In exploring the viability of a programmable sorbic acid derivative, it was envisaged that the expansion of the β-boryl acrylate framework from a C_3 to a C_5 core would allow the C(sp^2)-B bond to be leveraged in the development of a directional alkene isomerization process.[7,8]

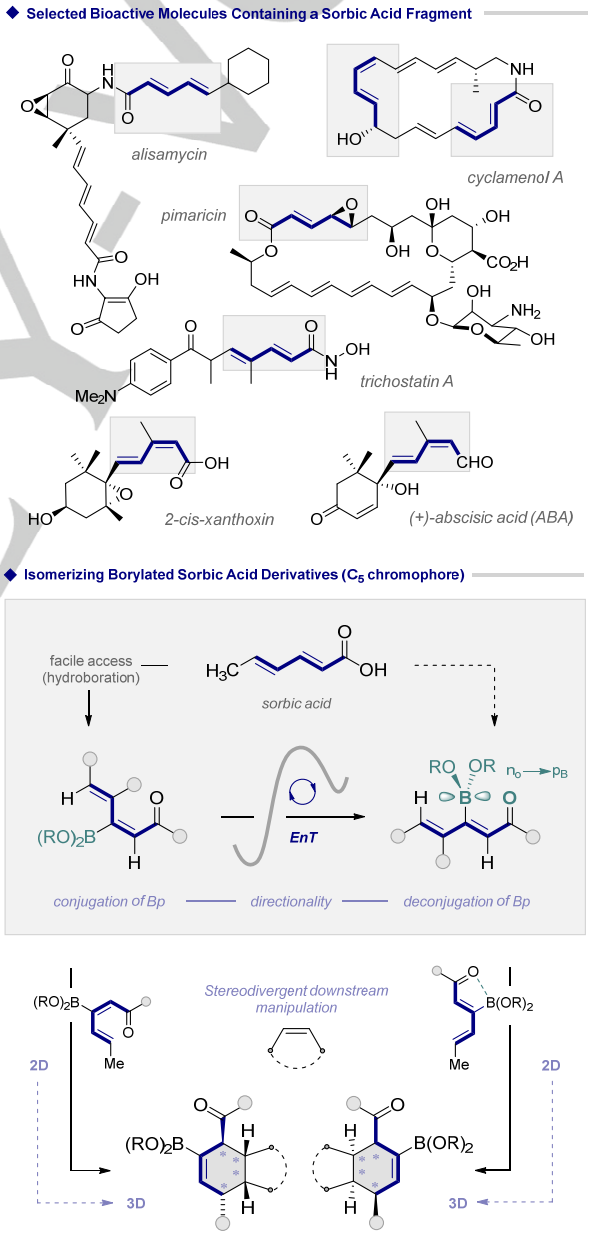

Figure 1. Top: Selected natural products containing (modified) sorbic acid fragments. Middle: Conceptual paradigm for the isomerization of a borylated 1,3-diene based on sorbic acid. Bottom: Stereospecific translation of 2D stereochemical information to 3D.

10.1002/anie.202404233

RESEARCH ARTICLE

This paradigm would also provide a scaffold with a traceless group for subsequent Suzuki-Miyaura cross-coupling,[9] where the boron unit would assist in pre-organising the terminal alkene through minimisation of non-bonding interactions. Whilst alkyne hydroboration would deliver the boron substituent opposite to the carbonyl group in the starting material, isomerization via selective energy transfer catalysis[10,11] would generate the formal *anti*-hydroboration product[12] to be generated in an operationally simple manner. Achieving stereodivergence through the intervention of a small molecule energy transfer catalyst requires that the triplet energies of the two isomers are meaningfully distinct.[13] Therefore, success would be conditional on the boron *p*-orbital being intimately involved in the π-system in the starting isomer, but rotating 90° out of conjugation in the product. This form of chromophore bifurcation would be achieved through a stabilising ($n_O \rightarrow p_B$) interaction[7,13,14,15] which would elevate the triplet energy and enable $Z \rightarrow E$ directionality. However, introducing a one atom stereoelectronic regulatory mechanism to partition a conjugated π-system for regio- and stereo-selective diene isomerization has not yet been demonstrated.[16,17]

Results and Discussion

To validate the regio- and stereo-selective isomerization of a C_5-borylated sorbic acid analog using selective energy transfer catalysis, substrate ***Z*-1** was prepared in a concise manner via alkyne hydroboration (please see the Supporting Information).

Table 1. Optimization of the transformation of ***Z*-1** to ***E*-1**.[a]

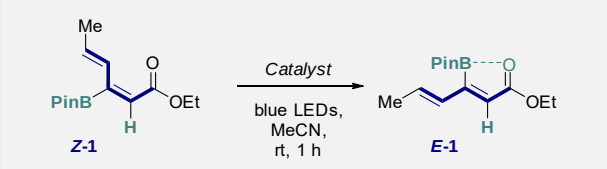

Entry	Catalyst	E_T (kJ/mol)	LEDs (nm)	T (°C)	Loading (mol%)	yield (%)	*E/Z*
1	Thioxanthone	265	402	rt	5.0	98	54:46
2	$[Ir(dF(CF_3)ppy)_2(dtbbpy)]PF_6$	251	435	rt	5.0	96	55:45
3	*fac*-Ir(ppy)$_3$	231	435	rt	5.0	67	65:35
4	riboflavin	209	402	rt	5.0	90	64:36
5	$[Ir(ppy)_2(dtbbpy)]PF_6$	205	435	rt	5.0	51	65:35
6	$[Ru(bpy)_3](PF_6)_2$	195	435	rt	5.0	93	88:12
7	$[Mes\text{-}Acr]ClO_4$	187	435	rt	5.0	55	63:37
8	anthracene	178	365	rt	5.0	98	8:92
9	-	-	402	rt	-	>98	<1:99
10	$[Ru(bpy)_3](PF_6)_2$	195	-	rt	5.0	>98	<1:99
11	$[Ru(bpy)_3](PF_6)_2$	195	400	0	5.0	95	91:9
12	$[Ru(bpy)_3](PF_6)_2$	195	400	-10	5.0	97	93:7
13	$[Ru(bpy)_3](PF_6)_2$	195	400	-20	5.0	97	94:6
14	$[Ru(bpy)_3](PF_6)_2$	195	400	-30	5.0	97	95:5
15	$[Ru(bpy)_3](PF_6)_2$	195	400	-40	5.0	97	95:5
16	$[Ru(bpy)_3](PF_6)_2$	195	400	-30	2.5	97	95:5
17	**$[Ru(bpy)_3](PF_6)_2$**	**195**	**400**	**-30**	**1.0**	**97**	**95:5**

[a] Standard reaction conditions: ***Z*-1** (0.1 mmol), catalyst (mol%), MeCN (3.3 mL), blue LEDs, 60 mins, Ar atmosphere. Yields and *E*:*Z* ratios were determined by ^{1}H NMR using dibromomethane as an internal standard. The *Z/E* assignment of the alkene follows IUPAC nomenclature and reflects the priority C > B.

The conversion of ***Z*-1** to ***E*-1** was then explored with a range of common photosensitizers that spanned the triplet range from 265 to 178 kJ•mol^{-1} (Table 1, entries 1-8).[18] This investigation led to the identification of $[Ru(bpy)_3](PF_6)_2$ as being effective in enabling the reaction of interest (*E/Z* 88:12). Importantly, removal of the catalyst or the light source from the reaction vessel completely suppressed the reaction (entries 9 and 10), which is in line with the working hypothesis (Figure 1).

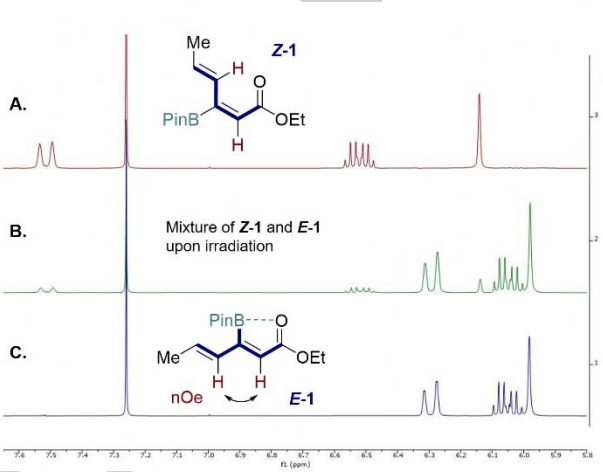

Figure 2. ^{1}H NMR (400 MHz, $CDCl_3$) analyses of the starting isomer ***Z*-1** (red, A), the reaction mixture after 60 minutes (green, B), and the product ***E*-1** (blue, C).

To further enhance the stereoselectivity of the reaction, the temperature was systematically lowered from ambient temperature to -30 °C; this led to a consistent enhancement in the *E/Z* ratio from 88:12 to 95:5 (entries 11 to 14).[19] Further decreasing the temperature to -40 °C (entry 15) did not improve the outcome and encroached on the melting point of acetonitrile (-45 °C). Finally, the catalyst loading was reduced to 2.5 mol% (entry 16) and then to 1 mol% (entry 17) without any detrimental impact on reaction efficiency. Changes in the reaction medium did not lead to an improvement of these optimized condition (please see the Supporting Information). Gratifyingly, the isomerization of ***Z*-1** to ***E*-1** occurred smoothly and this is evident from the ^{1}H NMR analysis of the starting material (Fig. 2A, red, ***Z*-1**), reaction mixture (Fig. 2B, green) and the product (Fig. 2C, blue, ***E*-1**). In addition to securing the configuration of the product ***E*-1** by nOe analysis, it was possible to unequivocally establish the structure of both isomers by single crystal X-ray diffraction analysis (*vide infra*).[20] Having identified conditions to enable the regio- and stereo-selective isomerization of borylated 1,3-diene ***Z*-1** under the auspices of Ru-photocatalysis, attention was turned to exploring the scope and limitations of the transformation (Figure 3). Initially, the impact of modifying the carbonyl substituent was investigated relative to compound ***E*-1**. Gratifyingly, the introduction of electronically and sterically modulated groups was well tolerated (***E*-2-4**, up to 96:4 *E/Z*). Weinreb amides (e.g. ***E*-5**) and benzyl protected amides such as ***E*-6** were also found to be tolerated under the reaction conditions.

10.1002/anie.202404233

WILEY-VCH

RESEARCH ARTICLE

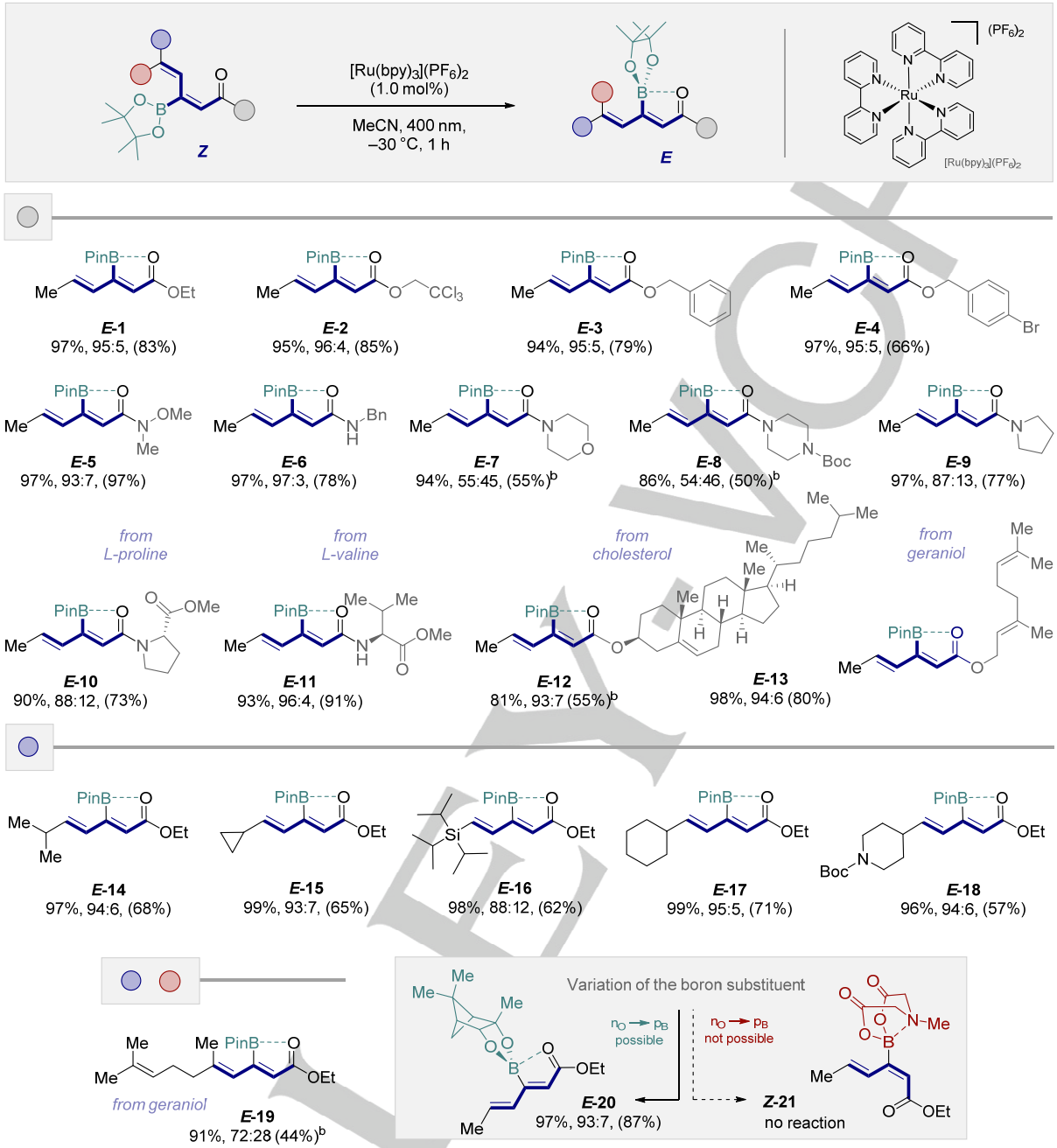

Figure 3. Exploring the scope and limitation of the isomerization of borylated 1,3-dienes via Ru-photocatalysis. [a] Standard reaction conditions: *Z*-isomer, catalyst (1.0 mol%), MeCN, 400 nm light, 1 hour, –30 °C, Ar atmosphere. Yields and *E*:*Z* ratios were determined by ^{1}H NMR using dibromomethane as an internal standard. Isolated yields given in parenthesis. [b] Reaction time: 3.0 hour.

The morpholine and 1,4-piperazine derivatives ***E*-7** and ***E*-8** proved more challenging. This may be a consequence of a reduced $n_O \rightarrow p_B$ interaction. It is interesting to note that reducing the ring size of the amide from 6 → 5, as in the case of ***E*-9**, enabled the selectivity to be increased to 87:13. This is fully in-line with the notion that 1,3-allylic strain has an influence on amide pyramidalization[21] and this manifests itself in stereoselectivity. Similar results were observed with the L-proline adduct ***E*-10**, whilst employing an acyclic amide such as the L-valine derivative ***E*-11** enabled high levels of stereoselectivtivity to be restored (94:6). Finally, the incorporation of more complex cholesterol and geraniol side chains had no impact on reaction selectivity (up to 94:6 *E*/*Z* for ***E*-12** and ***E*-13**). Variation of the terminal alkene unit was generally well tolerated as is exemplified by the replacement of the methyl unit (in ***E*-1**) by isopropyl and cyclopropyl groups (***E*-14** and ***E*-15**, 94:6 and 93:7, respectively). The introduction of a TIPS group was also compatible with the general reaction conditions (***E*-16**), as were the cyclohexyl and Boc-protected piperidine groups (***E*-17** and ***E*-18**, 95:5 and 94:5, respectively). The terminal 1,1-disubstituted geraniol derivative ***E*-19** proved more challenging (72:28); this is likely a consequence of allylic strain between the methyl group and the BPin substituent. To gain support for the importance of the $n_O \rightarrow p_B$ interaction, the BPin was replaced by two alternatives in which the boron *p*-orbital was either vacant or occupied. To represent the former

10.1002/anie.202404233

case, ***E*-20** was generated in 97% (93:7). In contrast, the BMIDA derivative ***Z*-21** proved recalcitrant to isomerization.

To provide structural support for the importance of this stabilizing $n_O \rightarrow p_B$ interaction in imparting directionality to this dienone isomerization, X-ray structural analysis of ***Z*-2** and ***E*-2** was performed (Figure 4). In the case of the starting isomer ***Z*-2**, it is evident that the boron *p*-orbital is conjugated with the dieneone chromophore (Figure 4, top). However, in the product isomer ***E*-2**, regio- and stereo-selective isomerization of the central π-bond is accompanied by a rotation of the C(sp^2)-B bond with the carbonyl oxygen and boron atoms being separated by 2.66 Å, which is shorter than the sum of the van der Waals radii (3.35 Å). The expected planarity at the boron center is confirmed by the sum of the angles (359.3°) (Figure 4, bottom). This subtle, one-atom difference causes chromophore bifurcation and allows the regio- and stereo-selectivity of the transformation to be placed on a structural foundation.

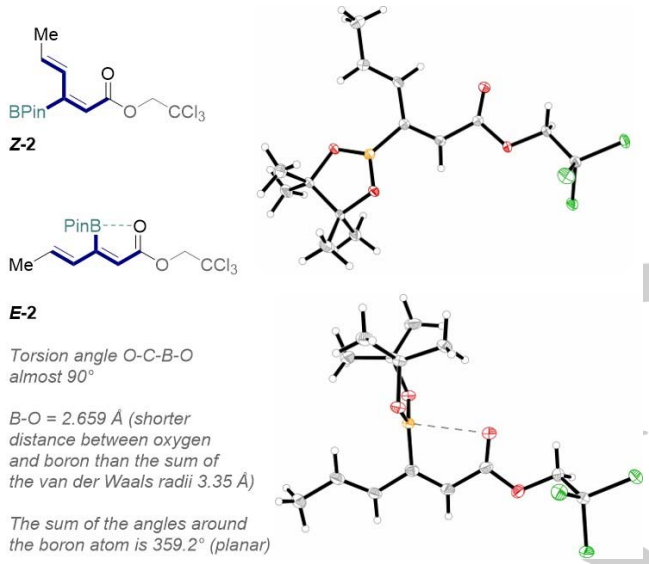

Figure 4. X-ray crystal structure analyses of ***Z*-2** and ***E*-2** (CCDC numbers 2326271 and 2326272, respectively). Thermal ellipsoids are set at 50% probability.[20]

To illustrate the synthetic utility of this isomerization in the construction of highly substituted Diels-Alder adducts bearing a BPin handle, ***Z*-1** and ***E*-1** were independently processed to the bicyclic products **(±)-22** (*anti*) and **(±)-23** (*syn*), respectively (Figure 5).[22] This proved to be facile enabling these stereoisomer products to be isolated in 77% and 65% yield, respectively. The relative configurations of the four contiguous centers in each product was unequivocally established by single crystal X-ray analysis (Figure 5, bottom).[20] To provide additional support for a selective energy transfer paradigm, a series of mechanistic investigations were performed (Figure 6). As expected, Stern-Volmer quenching studies confirmed that a collisional process was operational in which ***Z*-1** selectively quenched the excited state Ru photocatalyst (Figure 6a). Cyclic voltammetry (CV) was employed to demonstrate that neither the *Z* nor the *E* isomer of the borylated diene match the reduction potential of the employed Ru-photocatalyst (Figure 6b).

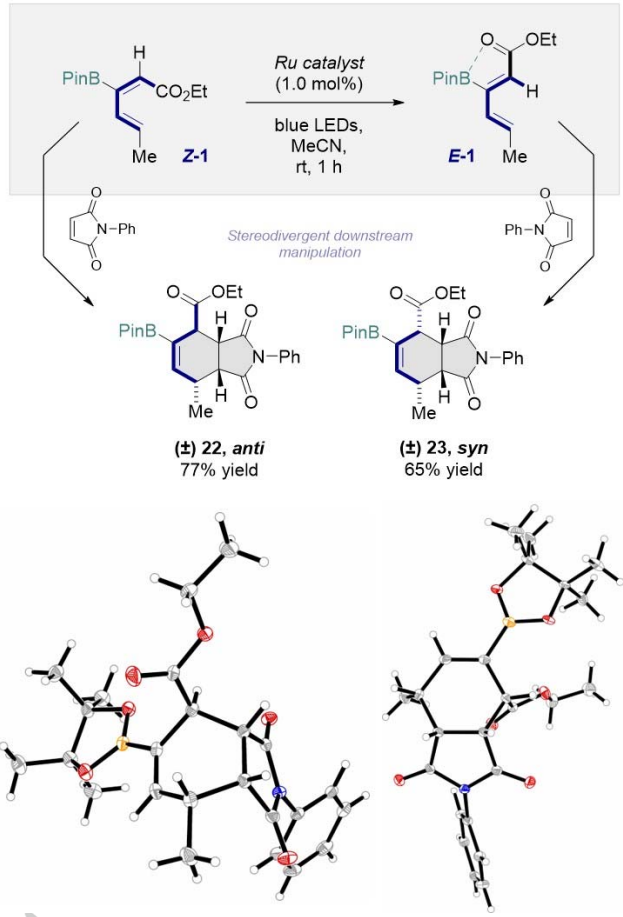

Figure 5. Top: Merging 1,3-diene isomerization with stereospecific Diels-Alder cycloaddition to access diastereomers **(±)-22** (*anti*) and **(±)-23** (*syn*). Reaction conditions: 1,3-diene (0.24 mmol), dienophile (0.2 mmol), toluene (2.0 mL), 16 hours, 115 °C, Ar atmosphere. Isolated yields indicated. Bottom: Rigorous proof of the relative stereochemical relationship by single crystal X-ray diffraction [**(±)-22** (CCDC number 2326273) and **(±)-23** (CCDC number 2326274)]. Thermal ellipsoids are set at 50% probability.[20]

Both ***Z*-1** and ***E*-1** have have reduction potentials lower than -1.8 V vs SCE whereas the excited photocatalyst has a reduction potential of -0.81 V vs SCE in the oxidative quenching mode. Therefore, electron transfer processes can be excluded.

To exclude the possibility of direct excitation of either ***Z*-1** or ***E*-1**, and further support an energy transfer paradigm, the absorption spectra of both isomers were measured in CH_3CN (0.05 mmol) and compared with the emission spectra of the LEDs (ca 370-450 nm) (Figure 6c, please also see Figure S12 in the Supporting Information). This revealed that there was no spectral overlap, which is fully in line with the control experiment in the absence of the catalyst (Table 1, entry 9). As is illustrated in Figure 6d, the stereoselectivity of the reaction shows a clear temperature dependence and this manifests itself in a linear relationship between the $\log_{10}(E{:}Z)$ ratio versus 1/T (K^{-1}) (please see Table 1, entries 10-15).

10.1002/anie.202404233

RESEARCH ARTICLE

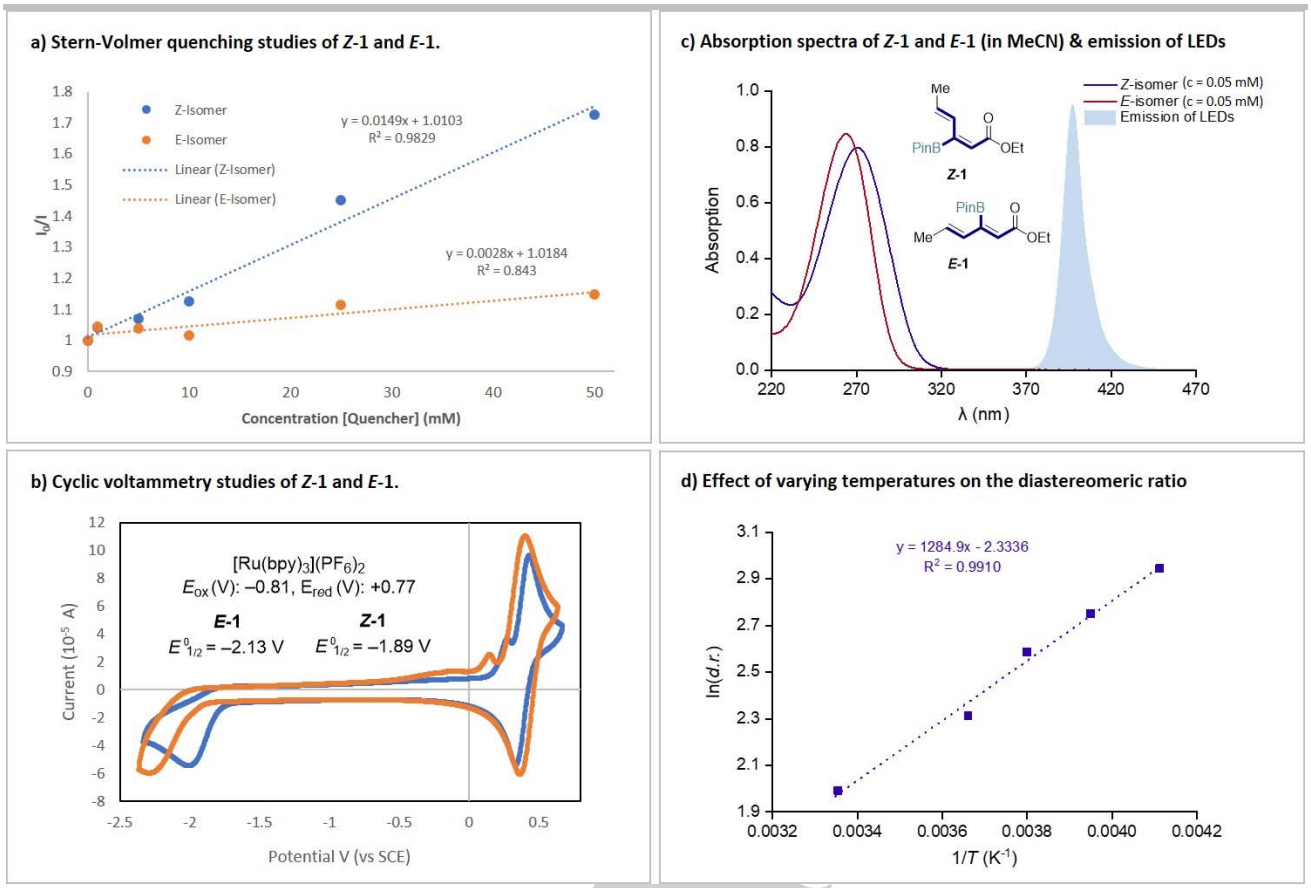

Figure 6. Selected mechanistic experiments (a) Stern-Volmer quenching experiments with ***Z*-1** and ***E*-1**; (b) cyclic voltammetry versus SCE; (c) absorption spectra of ***Z*-1** and ***E*-1** (in MeCN) and emission of the LED used in the study; (d) Exploring the impact of temperature on the *Z*:*E* selectivity.

To demonstrate the utility of the method when unified with a subsequent stereospecific cross-coupling event, ***Z*-1** was isomerized to ***E*-1** and then both isomers were independently processed to the respective trienes (**24** and **25**, 61 and 73%). Furthermore, reduction to forge the pharmaceutically relevant boracycle[23] proved facile enabling **26** to be isolated in 77% yield (Figure 7, top). Augmentation of the chromophore to include a terminal phenyl ring was explored (***E*-27**) in the hope that an orthogonal, regioselective isomerization might be developed (Figure 7, bottom). However, upon Ru-enabled photosensitization, the β-boryl acrylate fragment isomerized (**28**) and this led to a highly efficient [2+2] cycloaddition (**29**, 90% yield): this is evident from the relative configuration of the ester and BPin substituents in the highly congested cyclobutane ring (Figure 7, see the X-ray analysis).[20]

Conclusions

Under the auspices of Ru-photocatalysis, a regio- and stereoselective isomerization of ambiphilic, borylated 1,3-dienes has been achieved. Motivated by the prevalence of C_5 sorbic acid motifs in the bioactive small molecule repertoire, a borylated scaffold has been developed in which the traceless BPin group has been leveraged to subtly bifurcate the chromophore in the product. The reaction is operationally simple (complete in 60 minutes), requires low catalyst loadings (1 mol%) and is highly selective (up to *E*:*Z* >95:5). Mechanistic studies support the involvement of a selective energy transfer process, and crystallographic analyses provide a structural foundation for selectivity based on a very subtle 90° rotation of the C(sp^2)-B bond. The synthetic utility of the method has been demonstrated in stereospecific cycloaddition reactions to access densely substituted, alkenyl BPin-containing cyclohexenes. It is envisaged that this methodology will be highly enabling in complex polyene synthesis and analog design.

Acknowledgements

We acknowledge generous financial support from the University of Münster, the Deutsche Forschungsgemeinschaft (German Research Foundation - GRK2678-437785492), the European Union H2020 research and innovation program under the Marie S. Curie Grant Agreement (PhotoReAct, No 956324, BK), the Alexander von Humboldt Foundation (Fellowship to AM) and the Fonds der Chemischen Industrie (Kekulé Fellowship to J.S.).

Keywords: boron, diene, energy transfer catalysis, isomerization, stereoselectivity

10.1002/anie.202404233

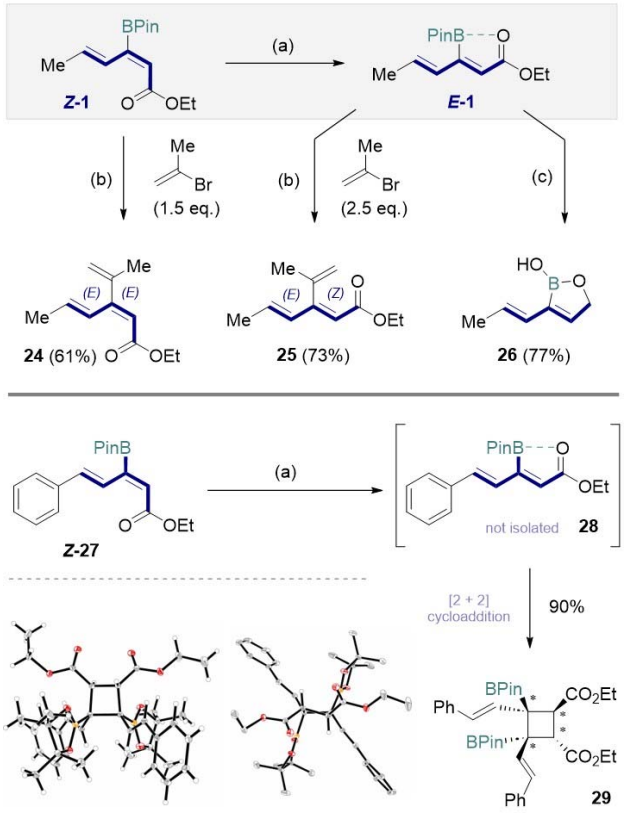

Figure 7. Selected derivatization reactions of borylated diene ***Z*-1, *E*-1 and *E*-27**. Conditions: (a) $[Ru(bpy)_3](PF_6)_2$ (1 mol%), MeCN, 400 nm, -30 °C, 1 h; (b) $Pd(dppf)Cl_2$ (2 mol%), Na_2CO_3 (2.0 eq.), 1,4-dioxane/H_2O (5:1) 90 °C, 2 h; (c) NaBH4 (2.5 eq.), EtOH, ambient temperature, 2.5 h. CCDC number 2335038. Thermal ellipsoids are set at 50% probability.[20]

References

[1] a) C. Thirsk, A. Whiting, *J. Chem. Soc., Perkin Trans 1* **2002**, 999-1023; b) P. Hubert, E. Seibel, C. Beemelmanns, M.-M. Campagne, R. M. de Figueiredo, *Adv. Synth. Catal.* **2020**, *362*, 5532-5575.

[2] a) C. Dugave, L. Demange. *Chem. Rev.* **2003**, *103*, 2475-2532; b) L. F. Maia, R. F Fernandez, G. Lobo-Hajdu, L. F. C. de Oliveira, *Phil. Trans. R. So. A* **2014**, *372*, 20140200; c) P. D. Kiser, M. Golczak, K. Palczewski, *Chem. Rev.* **2014**, *114*, 194–232; d) C. Chatgilialoglu, C. Ferreri, M. Melchiorre, A. Sansone, A. Torreggiani, *Chem. Rev.* **2014**, *114*, 255–284; e) S. Martinez-Cuesta, S. A. Rahman, J. M. Thornton, *Proc. Natl. Acad. Sci. U.S.A.* **2016**, *113*, 1796-1801; f) C. M. Pearson, T. N. Snaddon, *ACS Cent. Sci*. **2017**, *3*, 922-924.

[3] a) A. Eschenmoser, D. Arigoni, *Helv. Chim. Acta* **2005**, *88*, 3011-3048; b) J. W. Cornforth, *Pure Appl. Chem*. **1961**, *2*, 607-630; c) Z. Yin, J. S. Dickschat, *Nat. Prod. Rep.* **2021**, *38*, 1445-1468.

[4] a) R. S. Stoll, S. Hecht, *Angew. Chem. Int. Ed*. **2010**, 49, 5054-5075; b) M. Kathan, S. Hecht, *Chem. Soc. Rev.* **2017**, *46*, 5536-5550; c) J. J. Molloy, T. Morack, R. Gilmour, *Angew. Chem. Int. Ed.* **2019**, *58*, 13654-13664.

[5] E. M. Woerly, J. Roy, M. D. Burke, *Nat. Chem*. **2014**, *6*, 484-491.

[6] K. C. Nicolaou, S. A. Snyder, T. Montagnon, G. Vassikikogiannakis, *Angew. Chem. Int. Ed*. **2002**, *41*, 1668-1698.

[7] For application to C_3 alkene fragments, see a) M. Wienhold, B. Kweon, C. McLaughlin, M. Schmitz, T. J. B. Zähringer, C. G. Daniliuc, C. Kerzig and R. Gilmour, *Angew. Chem. Int. Ed.* **2023**, e202304150; b) J. J. Molloy, M. Schäfer, M. Wienhold, T. Morack, C. G. Daniliuc and R. Gilmour, *Science* **2020**, *369*, 302-306. Please also a recent report on borylated ethyl acetoacetate building blocks: A. Trofimova, B. White, D. B. Diaz, M. J. Širvinskas, A. Lough, T. Dudding, A. K. Yudin, *Angew. Chem. Int. Ed*. **2024**, e202319842.

[8] For examples of C_1 organoboron fragments see, a) J. D. St. Denis, Z. He, A. K. Yudin, *ACS Catal*. **2015**, *5*, 5373–5379; b) A. Holownia, C.-H. Tien, D. B. Diaz, R. T. Larson, A. K. Yudin, *Angew. Chem. Int. Ed*. **2019**, *58*, 15148-15153; c) Y. M. Ivon, I. V. Mazurenko, Y. O. Kuchkovska, Z. V. Voitenko, O. O. Grygorenko, *Angew. Chem. Int. Ed*. **2020**, *59*, 18016-18022.

[9] N. Miyaura, A. Suzuki, *Chem. Rev*. **1995**, *95*, 2457-2483; b) A. J. J. Lennox, G. C. Lloyd-Jones, *Chem. Soc. Rev.* **2014**, *43*, 412-443; c) J. W. B. Fyfe, A. J. B. Watson, *Chem* **2017**, *3*, 31-55.

[10] a) T. Neveselý, M. Wienhold, J. J. Molloy and R. Gilmour, *Chem. Rev.* **2022**, *122,* 2650-2694; b) Q. -Q. Zhou, Y. -Q. Zou, L. -Q. Lu, W. -J. Xiao, *Angew. Chem. Int. Ed.* **2019**, *58*, 1586-1604; c) J. B. Metternich, R. Gilmour, *Synlett* **2016**, *27*, 2541–2552.

[11] T. J. B. Zähringer, M. Wienhold, R. Gilmour and C. Kerzig, *J. Am. Chem. Soc.* **2023**, *145,* 21576-21586.

[12] For selected examples, see: a) S. Xu, Y. Zhang, B. Li, S.-Y. Liu, *J. Am. Chem. Soc*. **2016**, *138*, 14566-14569; b) M. Nogami, K. Hirano, M. Kanai, C. Wang, T. Saito, K. Miyamoto, A. Muranaka, M. Uchiyama, *J. Am. Chem. Soc*. **2017**, *139*, 12358-12361; c) K. Nagao, A. Yamazaki, H. Ohmiya, M. Sawamura, *Org. Lett.* **2018**, *20*, 1861-1865; d) R. J. Grams, R. G. Fritzemeier, C. Slebodnick, W. L. Santos, *Org. Lett.* **2019**, *21*, 6795-6799; e) M. Nogami, K. Hirano, K. Morimoto, M. Tanioka, K. Miyamoto, A. Muranaka, M. Uchiyama, *Org. Lett*. **2019**, *21*, 3392-3395; f) T. Brégent, J. Bouillon, T. Poisson, *Chem. Eur. J.* **2021**, *27*, 13966–13970; g) J. Corpas, M. Gomez-Mendoza, J. Ramírez-Cárdenas, V. A. De La Peña O'Shea, P. Mauleón, R. Gómez Arrayás, J. C. Carretero, *J. Am. Chem. Soc.* **2022**, *144*, 13006–13017; h) For an excellent review, see: A. Fürstner, *Isr. J. Chem*. **2023**, *63*, e202300004.

[13] For selected examples, see a) K. Singh, K.; S. J. Staig, J. D. Weaver, *J. Am. Chem. Soc.* **2014**, *136*, 5275–5278; b) J. B. Metternich, R. Gilmour, *J. Am. Chem. Soc*. **2015**, *137*, 11254-11257; b) J. B. Metternich, R. Gilmour, *J. Am. Chem. Soc.* **2016**, *138*, 1040–1045; c) J. B. Metternich, D. G. Artiukhin, M. C. Holland, M. von Bremen-Kühne, J. Neugebauer, R. Gilmour, *J. Org. Chem.* **2017**, 82, 9955–9977; d) W. Cai, H. Fan, D. Ding, Y. Zhang, W. Wang, *Chem. Commun.* **2017**, *53*, 12918 – 12921; e) T. Kurzawa, K. Harms, U. Koert, *Org. Lett.* **2018**, *20*, 1388-1391; f) J. J. Molloy, J. B. Metternich, C. G. Daniliuc, A. J. B. Watson, R. Gilmour, *Angew. Chem. Int. Ed.* **2018**, *57,* 3168-3172*;* g) S. I. Faßbender, J. J. Molloy, C. Mück-Lichtenfeld, R. Gilmour, *Angew. Chem. Int. Ed.* **2019**, *58*, 18619-18626; h) T. Neveselý, C. G. Daniliuc, R. Gilmour, *Org. Lett.* **2019**, *21*, 9724-9728; i) C. Onneken, K. Bussmann and R. Gilmour, *Angew. Chem. Int. Ed.* **2020**, *59*, 330-334.

[14] a) T. Neveselý, J. J. Molloy, C. McLaughlin, L. Brüss, C. G. Daniliuc, R. Gilmour, *Angew. Chem. Int. Ed.* **2022**, *61*, e202113600; b) M. Wienhold, J. J. Molloy, C. G. Daniliuc, R. Gilmour, *Angew. Chem. Int. Ed.* **2021**, *60*, 685-689; c) T. Hostmann, T. Nevesely, R. Gilmour, *Chem. Sci.* **2021**, *12*, 10643 - 10648.

[15] A. Marotta, C. E. Adams, J. J. Molloy, *Angew. Chem. Int. Ed.* **2022**, *61*, e202207067.

[16] R. A. Caldwell, M. Singh, M. *J. Am. Chem. Soc.* **1982**, *104*, 6121–6122.

[17] For selected examples of metal-catalyzed geometric diene isomerization, see a) F. Pünner, A. Schmidt, G. Hilt, *Angew. Chem. Int. Ed.* **2012**, *51*, 1270-1273; b) E. Kudo, K. Sasaki, S. Kawamata, K. Yamamoto, T. Murahashi, *Nat. Commun*. **2021**, *12*, 1473; c) W. Wang, S. He, Y. Zhong, J. Chen, C. Cai, Y. Luo, Y. Xia, *J. Org. Chem.* **2022**, *87*, 4712-4723.

[18] M. Montalti, A. Credi, L. Prodi, M. T. Gandolfi, M. T. *Handbook of Photochemistry*, 3rd ed.; CRC/Taylor & Francis: Boca Raton, **2006**.

[19] To perform the low temperature work, a set-up was used with a 400 nm LED as opposed to 435 nm.

[20] Deposition Numbers 2326271 (for ***Z*-2**), 2326272 (for ***E*-2**), 2326273 (for **22**), 2326274 (for **23**) and 2335038 (for **29**) contain the supplementary crystallographic data for this paper. These data are provided free of charge by the joint Cambridge Crystallographic Data Centre (CCDC) and Fachinformationszentrum Karlsruhe Access Structures service.

10.1002/anie.202404233

[21] G. Meng, J. Zhang, M. Szostak, *Chem. Rev*. **2021**, *121*, 12746-12783.

[22] a) G. Hilt, P. Bolze, *Synthesis* **2005**, 2091-2115; b) J. Pyziak, J. Walkowiak, B. Marciniec, *Chem. Eur. J*. **2017**, *23*, 3502-3541.

[22] K. Livingstone, M. Tenberge, F. Pape, C. G. Daniliuc, C. Jamieson, R. Gilmour, *Org. Lett.* **2019**, *21*, 9677-9680.

[23] a) R. Smoum, A. Rubinstein, V. M. Dembitsky, M. Srebnik, *Chem. Rev*. **2012**, *112*, 4156-4220; b) R. J. Grams, W. L. Santos, I. R. Scorei, A. Abad-García, C. A. Rosenblum, A. Bita, H. Cerecetto, C. Viñas, M. A. Soriano-Ursúa, *Chem. Rev*. **2024**, *124*, 2441–2511.

10.1002/anie.202404233

WILEY-VCH

RESEARCH ARTICLE

Entry for the Table of Contents

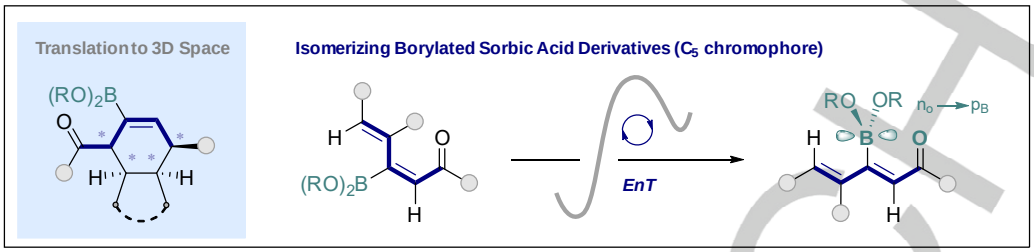

Sorbic acid-based C_5 units are ubiquitous in natural products. To complement biosynthesis algorithms, a regio- and stereo-selective isomerization of β-boryl-substituted dienes has been achieved by selective energy transfer catalysis (*E*:*Z* up to 99:1). Application of the method in stereospecific [4+2] and [2+2] cycloaddition processes is also disclosed to generate cyclic products with four contiguous stereocenters.

Institute and/or researcher X (Twitter) usernames: @GilmourLab @WWU_Muenster